Absolute chlorine and hydrogen atom quantum yield measurements in the 193.3 nm photodissociation of CH_3CFCl_2 (HCFC-141b)

Almuth Läuter,[a] Dhanya Suresh,[b] and Hans-Robert Volpp[a,*]

[a] Physikalisch-Chemisches Institut der Universität Heidelberg, Im Neuenheimer Feld 253, D-69120 Heidelberg, Germany

[b] Radiation Chemistry and Chemical Dynamics Division, Bhabha Atomic Research Centre, Mumbai 400-085, India

* Corresponding author:

Dr. Hans-Robert Volpp
Physikalisch-Chemisches Institut
Universität Heidelberg
Im Neuenheimer Feld 253
D-69120 Heidelberg, Germany
Fax: +49-(0)6221-545050
E-mail: aw2@ix.urz.uni-heidelberg.de

Abstract

The dynamics of chlorine and hydrogen atom formation in the 193.3 nm gas-phase laser photolysis of room-temperature 1,1-dichloro-1-fluoroethane, CH_3CFCl_2 (HCFC-141b), were studied by means of the pulsed laser photolysis/laser-induced fluorescence (LIF) "pump-and-probe" technique. Nascent ground state Cl($^2P_{3/2}$), spin-orbit excited Cl*($^2P_{1/2}$) as well as H(^2S) atom photofragments were detected under collision-free conditions by pulsed Doppler-resolved laser induced fluorescence measurements employing narrow-band vacuum ultraviolet probe laser radiation, generated *via* resonant third-order sum-difference frequency conversion of dye laser radiation in Krypton. Using HCl photolysis as a reference source of well-defined Cl($^2P_{3/2}$), Cl*($^2P_{1/2}$) and H atom concentrations, values for the chlorine atom spin-orbit branching ratio [Cl*]/[Cl] = 0.36 ± 0.08, the total chlorine atom quantum yield (Φ_{Cl+Cl^*} = 1.01 ± 0.14), and the H atom quantum yield (Φ_H = 0.04 ± 0.01) were determined by means of a photolytic calibration method. From the measured Cl and Cl* atom Doppler profiles the mean relative translational energy of the chlorine fragments could be determined to be $E_{T(Cl)}$ = 157 ± 12 kJ/mol and $E_{T(Cl^*)}$ = 165 ± 12 kJ/mol. The corresponding average values 0.56 and 0.62 of the fraction of total available energy channelled into CH_3CFCl + Cl/Cl* product translational energy was found to lie between the limiting values 0.36 and 0.85 predicted by a soft impulsive and a rigid rotor model of the $CH_3CFCl_2 \rightarrow CH_3CFCl$ + Cl/Cl* dissociation processes, respectively. The measured total chlorine atom quantum yield along with the rather small H atom quantum yield as well as the observed energy disposal indicates that direct C-Cl bond cleavage is the most important primary fragmentation mechanism for CH_3CFCl_2 after photoexcitation in the first absorption band.

I. INTRODUCTION

CH_3CFCl_2 (hydrochlorofluorocarbon:HCFC-141b) has been widely utilized as a replacement for $CFCl_3$ (chlorofluorocarbon:CFC-11) in the manufacturing process of closed cell insulating foams and for $CFCl_2CF_2Cl$ (CFC-113), which is used as a solvent in a variety of industrial processes.[1,2] As a consequence, measurements of tropospheric concentrations of this compound show a rapid increase since 1994.[3] Although its production has been stopped in 1996, and based on the revised Montreal Protocol its use will be phased out in developed countries by 2020,[4] the release into the atmosphere is expected to further increase in the coming few decades because of long term uses of the previously manufactured products.[5] Despite the fact that HCFCs such as CH_3CFCl_2, which contain one or more C-H bonds, can be oxidized by OH radicals in the troposphere,[6] they still have the potential to lead to noticeable chlorine transportation to the stratosphere[7] where they can be decomposed *via* radical reactions or photolytically after UV photon absorption in the 230-190 nm spectral region.[8,9] As a consequence, a number of reaction kinetics studies of CH_3CFCl_2 with atmospherically important radicals such as OH,[10] $O(^1D)$,[11] and Cl,[12] along with studies on the UV photodissociation dynamics of CH_3CFCl_2 were reported so far.[13,14]

In Ref. 13, ground state $Cl(^2P_{3/2})$, spin-orbit excited $Cl^*(^2P_{1/2})$ as well as $H(^2S)$ atom photofragment formation could be observed in the 193.3 nm photolysis of CH_3CFCl_2 and the relative product branching ratio [H]/[Cl + Cl*] along with the chlorine atom spin-orbit branching ratio [Cl*]/[Cl] were reported. In further experiments, the influence of selective methyl stretching vibrational excitation on the Cl atom spin-orbit branching[14] and the H atom versus chlorine atom product branching[14b] was investigated at a UV photolysis wavelength of 235 nm. The results of the latter studies demonstrated that vibrational excitation of the fundamental symmetric CH_3 ($1\nu_{CH}$) stretching mode leads to an increase in the chlorine atom spin-orbit branching ratio compared to that of vibrationally unexcited CH_3CFCl_2 molecules.[14a] A comparable increase in the chlorine atom spin-orbit branching ratio was observed in the 235 nm photolysis of CH_3CFCl_2 after pre-excitation of the second ($3\nu_{CH}$) and third ($4\nu_{CH}$) overtone of the symmetric CH_3 stretching

vibration while at the same time the relative H atom versus chlorine atom product branching was found to decrease upon overtone excitation.[14b] However, to the best of our knowledge no measurements of absolute photoproduct quantum yields have been reported so far for the UV photodissociation of CH_3CFCl_2 which are along with the corresponding optical absorption cross sections[8,9] a prerequisite for a detailed understanding of its UV photochemistry in the atmosphere.

In the present article we report results of absolute chlorine and H atom quantum yield measurements in the 193.3 nm photolysis of CH_3CFCl_2, which were performed using the pulsed laser photolysis (LP)/VUV laser-induced fluorescence (LIF) "pump-and-probe" technique. In the present study, the nascent Cl atom spin-orbit branching ratio, the absolute chlorine atom quantum yield Φ_{Cl+Cl^*}, and the absolute H atom quantum yield Φ_H were obtained by means of a photolytic calibration method employing HCl photolysis as a reference. In addition, the analysis of the measured Cl, Cl* and H atom Doppler profiles along with *ab initio* calculations, carried out to determine the heat of formation of the CH_3CFCl_2 parent molecule and the CH_3CFCl radical, allowed to derive information about the energy partitioning in the Cl, Cl* and H atom forming photofragmentation step. Primary dissociation mechanisms for the formation of chlorine and H atoms will be discussed.

II. EXPERIMENT AND THEORETICAL CALCULATIONS

The present photodissociation experiments were carried out in a flow cell at mTorr level pressures using a LP/VUV-LIF pump-probe setup similar to the one previously used to study the chlorine and H atom formation dynamics in the UV photodissociation of CH_3CF_2Cl (HCFC-142b).[15,16].

CH_3CFCl_2 (ABCR-Chemicals, purity > 99.7%) was pumped through the cell at room temperature. According to the manufacturer the impurity consists of CH_3CF_2Cl and CH_3CF_3 (HFC-143a), with the latter compound having a negligible absorption at 193.3 nm. For CH_3CF_2Cl the room-temperature optical absorption cross section at 193.3 nm is $\sigma_{CH_3CF_2Cl} = 0.58 \times 10^{-20}$ cm^2,[16,17] which is considerably lower than the corresponding absorption cross section of CH_3CFCl_2 ($\sigma_{CH_3CFCl_2} = 5.58 \times 10^{-19}$ cm²) recommended in Ref. 8c. Because the impurity level is less than 0.3%, contributions from the photolysis of CH_3CF_2Cl can be neglected.

In the photodissociation experiments the CH_3CFCl_2 pressure in the cell was typically 9-23 mTorr, for the calibration measurements HCl (Messer Griesheim, 99.99%) was flowed through the reaction cell at pressures of typically 9-72 mTorr. The pressure in the cell was monitored by an MKS-Baratron. Flow rates were regulated by calibrated mass flow controllers and were maintained at high enough rates to ensure renewal of the gases between successive laser shots at a laser repetition rate of 6 Hz. The unpolarized output of an ArF excimer laser (193.3 nm emission wavelength, pulse duration 15–20 ns) was used as a "pump" laser to dissociate the CH_3CFCl_2 parent molecules as well as HCl. Pump laser intensities were typically between 2-10 mJ/cm^2.

For LIF detection of Cl, Cl* and H atoms, narrow-band VUV "probe" laser radiation, tunable in the wavelength region 133.5–136.4 nm and around the H atom Lyman-α transition (121.567 nm) was generated by resonant third-order sum-difference frequency conversion ($\omega_{VUV} = 2\omega_R - \omega_T$) of pulsed dye laser radiation (pulse duration 15–20 ns) in Kr and in a phase-matched Kr/Ar mixture, respectively[18]. In the four-wave mixing process the frequency ω_R (λ_R = 212.55 nm) is two-photon resonant with the Kr 4p-5p (1/2, 0) transition. For chlorine atom LIF detection the second frequency ω_T could be tuned from 480 nm to 521 nm to cover the four allowed

Cl($4s^2P_{j'}$ ← $3p^2P_{j''}$; j´ =´1/2, 3/2 ← j´´ = 1/2, 3/2) transitions.[19] Ground-state Cl($^2P_{3/2}$) and excited-state Cl*($^2P_{1/2}$) atoms were detected *via* the (j´ = j´´)-transitions, which have the highest transition probabilities $f_{3/2,3/2}$ = 0.114 and $f_{1/2,1/2}$ = 0.088, respectively[20]. For H atom LIF detection *via* the ($2p\ ^2P \leftarrow 1s\ ^2S$) Lyman-α transition ω_T could be tuned from 844 nm to 846 nm. The fundamental laser radiation was obtained from two tunable dye lasers, simultaneously pumped by a XeCl excimer laser. The first dye laser was utilized to provided ω_T using Coumarin 307 dye in case of the Cl, Cl* LIF measurements and Styryl 9 dye for the H atom LIF detection. The second dye laser was operated with Coumarin 120 to generate light with a wavelength of 425.10 nm from which ω_R was obtained by frequency doubling with a BBO II crystal. The VUV light generated in the four-wave mixing process was carefully separated from the unconverted laser radiation by a lens monochromator followed by a light baffle system (for details see e.g. Ref. 21). Maximum VUV pulse energies up to 25 μJ can be achieved with this four-wave mixing method.[22] In the present study, however, the actual pulse energies were considerably lower due to absorption in the cell windows and optics. In all experiments the actual VUV probe laser intensity was reduced until a linear intensity dependence of the Cl, Cl* and H atom LIF signal was obtained. The bandwidth (FWHM) of the VUV probe laser radiation was determined to be ~0.3 cm^{-1} by measuring Doppler profiles of chlorine and H atoms generated in the 193.3 nm photolysis of HCl under thermalized conditions.

The VUV probe beam was aligned to overlap the photolysis beam at right angles in the viewing region of a LIF detector. The delay time between the photolysis and probe laser pulses was controlled by a pulse generator and monitored on a fast oscilloscope. In the Cl and Cl* formation dynamics measurements, the delay time between pumping and probing was kept short enough, typically 80–150 ns (with a time jitter of about ± 10 ns), to allow the collision-free detection of the nascent Cl and Cl* atoms produced in the CH_3CFCl_2 and HCl photolysis. As outlined in Ref. 16, these delay times were chosen to avoid any time-overlap between pump pulse and VUV probe laser pulse, which could results in unwanted multi-photon dissociation processes. Under the described experimental conditions, relaxation of Cl* by quenching as well as fly-out of

Cl, Cl* atoms and secondary reactions with CH_3CFCl_2 and HCl were negligible.

In the H atom formation dynamics studies, the delay time between pumping and probing was kept at 80–100 ns. As in our previous CH_3CF_2Cl and HCl photolysis studies, the quality of the spatial overlap of the pump and the H atom probe laser beam was carefully checked in order to ensure that no photolytically produced "fast" H atoms escape the detection region during the delay times used in the experiments (for details see Ref. 15).

Cl, Cl* and H atom LIF signals were detected through band pass filters, ARC model 130-B-1D, and 122-VN-1D, respectively, by a solar blind photomultiplier positioned at right angles to both pump and probe laser beams. The VUV probe laser beam intensity was monitored after passing through the reaction cell. As the VUV probe laser beam itself produced appreciable Cl, Cl* and H atom LIF signals *via* photolysis of CH_3CFCl_2 and HCl, respectively, it was necessary to subtract these "background" Cl, Cl* and H atoms from the Cl, Cl* and H atoms produced in the 193.3 nm photolysis of CH_3CFCl_2 and HCl. Therefore, an electronically controlled mechanical shutter was inserted into the photolysis beam path, such that at each point of the Cl, Cl* and H atom fluorescence excitation spectra, the signal could first be 30 times averaged with the shutter opened and again be 30 times averaged with the shutter closed. Finally a point-by-point subtraction procedure was adopted,[23] to obtain directly and on-line a LIF signal representing the contribution from Cl, Cl* and H atoms generated solely by the 193.3 nm photolysis laser pulse. The Cl, Cl* and H LIF signals, the VUV probe and photolysis laser intensity (the latter was monitored by a photodiode) were recorded with a boxcar system and transferred to a personal computer where the LIF signals were normalized to both pump and probe laser intensities. In the experiments special care was taken that the Cl, Cl* and H atom signals generated by the 193.3 nm photolysis laser pulse showed a linear dependence on the pump (see e.g. Fig. 1) and probe laser intensity.

In the present work the G2(MP2) method[24] of the GAUSSIAN-98 *ab initio* program package[25] was used for a direct calculation of heats of formation $\Delta_f H_{298}$ for the CH_3CFCl_2 parent molecule and for the CH_3CFCl fragment. For both species no experimental values are available. In

case of CH_3CFCl_2 a value of $\Delta_fH^o_{298}$ = -335.1 kJ/mol was reported in Ref. 26, which was estimated from available literature values of $\Delta_fH^o_{298}$ for CH_3CCl_3, CH_3CF_2Cl, and CH_3CF_3 employing a nonlinear fit procedure. The latter value was found to be in good agreement with the value $\Delta_fH^o_{298}$ = -333.3 kJ/mol calculated by Melius with the BAC-MP4 method.[27] The value of $\Delta_fH^o_{298}$ = -358.6 kJ/mol obtained for CH_3CFCl_2 in the present G2(MP2) calculations, however, deviates significantly from the results of the two previous calculations (for the CH_3CFCl radical the present G2(MP2) calculations yielded a value $\Delta_fH^o_{298}$ = -126.2 kJ/mol). Large deviations in the heats of formation of fluorinated and chlorinated compounds calculated by the G2(MP2) method were mentioned in Ref. 28. and attributed to systematic errors in the calculation of the atomization energies. It was found that the application of spin-orbit corrections can reduce the deviation from the experimental values in the case of chlorine compounds and it was concluded that G2 theory is not sufficiently accurate for compounds containing two or more F and Cl atoms. However, the application of isodesmic reaction schemes, where the number of each kind of bond stays the same, was found to significantly improve the accuracy of the heats of formation values obtained by direct theoretical method.[29] Therefore, G2(MP2) calculations on the isodesmic reaction scheme

$$CH_3CH_3 + CHFCl_2 \bullet CH_3CFCl_2 + CH_4 \qquad (1)$$

were carried out in the present work to calculate the enthalpy change from which Δ_fH_{298} for CH_3CFCl_2 could be derived employing the literature values for the experimental heats of formation of CH_3CH_3 (-84.1 kJ/mol),[28] $CHFCl_2$ (-283.3 kJ/mol),[30] and CH_4 (-74.9 kJ/mol).[28] With this approach a value of $\Delta_fH^o_{298}$ = -339.2 kJ/mol was obtained for CH_3CFCl_2, which is in reasonable agreement with the two values reported earlier.[26,27]

To derive an improved value for Δ_fH_{298} for CH_3CFCl a calculation on the isodesmic reaction

$$CH_3CH_2 + CHFCl_2 \bullet CH_3CFCl + CH_3Cl \qquad (2)$$

was performed using the experimental heats of formation of CH_3CH_2 (120.9 kJ/mol),[28] $CHFCl_2$

(-283.3 kJ/mol),[30] and CH_3Cl (-83.7 kJ/mol).[30] The latter calculation yielded a value of $\Delta_f H^o_{298}$ = -119.1 kJ/mol for the CH_3CFCl radical. The $\Delta_f H^o_{298}$ values obtained for CH_3CFCl_2 and CH_3CFCl *via* the isodesmic reactions (1) and (2), respectively, are listed in Table I along with available literature values of other possible photolysis products, which were used to calculate the reaction enthalpies $\Delta_r H^o_{298}$ of different dissociation channels and the corresponding values of the energies available to the products. With the $\Delta_f H^o_{298}$ values for CH_3CFCl_2 and CH_3CFCl of the present work along with the $\Delta_f H^o_{298}$ value reported in Ref. 31 for the Cl atom a value of $\Delta_r H^o_{298}$ = 341.4 kJ/mol for the C-Cl bond breaking reaction channel $CH_3CFCl_2 \rightarrow CH_3CFCl + Cl$ can be obtained, which is in good agreement with an estimated value of 351 ± 35 kJ/mol reported in Ref. 14c.

In the same way, the heat of formation value $\Delta_f H_{298}$ = 77.8 kJ/mol for the CHCFCl radical, for which to the best of our knowledge also no experimental value is available, was calculated employing the isodesmic reaction scheme

$$CHCH_2 + ¼\ CCl_4 + ¼\ CF_4 \bullet CHCFCl + ½\ CH_4 \qquad (3)$$

along with the known heats of formation of $CHCH_2$ (299.6 kJ/mol),[27] CCl_4 (-95.8 kJ/mol), CF_4 (-993 kJ/mol), and CH_4 (-74.9 kJ/mol).[28]

III. RESULTS

A. [Cl*]/[Cl] spin-orbit branching ratio and primary quantum yields for chlorine and hydrogen atom formation

Primary quantum yields Φ_{Cl} for Cl and Φ_{Cl^*} for Cl* atom photofragment formation were measured separately by calibrating the Cl, Cl* atom signals $S_{Cl}(CH_3CFCl_2)$, $S_{Cl^*}(CH_3CFCl_2)$ obtained in the CH_3CFCl_2 photodissociation against the Cl, Cl* atom signals $S_{Cl}(HCl)$, $S_{Cl^*}(HCl)$ from well-defined Cl,Cl* atom number densities generated in the 193.3 nm photolysis of HCl (see Fig. 2). Values for the quantum yields Φ_{Cl} for Cl and Φ_{Cl^*} for Cl* formation in the photolysis of CH_3CFCl_2 were determined using equations (4a) and (4b), respectively:[16]

$$\Phi_{Cl} = \gamma_{Cl} \{S_{Cl}(CH_3CFCl_2)\, \phi_{Cl}\, \sigma_{HCl}\, p_{HCl}\} \; / \; \{S_{Cl}(HCl)\, \sigma_{CH_3CFCl_2}\, p_{CH_3CFCl_2}\}. \quad (4a)$$

$$\Phi_{Cl^*} = \gamma_{Cl^*} \{S_{Cl^*}(CH_3CFCl_2)\, \phi_{Cl^*}\, \sigma_{HCl}\, p_{HCl}\} \; / \; \{S_{Cl^*}(HCl)\, \sigma_{CH_3CFCl_2}\, p_{CH_3CFCl_2}\}. \quad (4b)$$

σ_{HCl} and $\sigma_{CH_3CFCl_2}$ are the optical absorption cross-sections of HCl and CH_3CFCl_2 at room temperature at 193.3 nm. S_{Cl} and S_{Cl^*} are the integrated areas under the measured Cl and Cl* atom Doppler profiles and p_{HCl} and $p_{CH_3CFCl_2}$ are the pressures of HCl and CH_3CFCl_2, respectively. ϕ_{Cl^*} = 0.40 and ϕ_{Cl} = 0.60 are the Cl and Cl* quantum yields in the 193.3 nm photolysis of HCl, which can be derived, because the photodissociation of HCl generates H + Cl(Cl*) products with a quantum yield of unity ($\phi_H = \phi_{Cl^*} + \phi_{Cl} = 1$), from the [Cl*]/[Cl] spin-orbit branching ratio, 0.67 ± 0.09, ratio reported in Ref. 16. For the HCl absorption cross section, the value $\sigma_{HCl} = (8.1 \pm 0.4) \times 10^{-20}$ cm^2 was used, which has been measured for the ArF excimer laser emission wavelength (193.3 nm)[32]. The latter value is in good agreement with the value of 8.26×10^{-20} cm^2 obtained by nonlinear interpolation from the recommended data[8(b)] given in Ref. 33. For the CH_3CFCl_2 absorption cross section the value $\sigma_{CH_3CFCl_2} = (5.58 \pm 0.11) \times 10^{-19}$ cm^2 derived from the data

recommended in Ref. 8c was employed.

The factors γ_{Cl^*}, and γ_{Cl} in Eqs. (4a) and (4b), respectively, are corrections accounting for the different degrees of absorption of the Cl ($\lambda_{probe} \approx 134.72$ nm) and Cl*($\lambda_{probe} \approx 135.16$ nm) VUV probe laser radiation by CH_3CFCl_2 and HCl. These absorption corrections were directly determined from the known distances inside the flow cell and the relative difference in the probe laser attenuation measured in the CH_3CFCl_2 and HCl photolysis runs. Under the present experimental conditions the absorption corrections were $\gamma_{Cl} = 0.94 \pm 0.05$ and $\gamma_{Cl^*} = 0.96 \pm 0.05$. The experimental data sets evaluated *via* Eqs. (4) to determine Φ_{Cl} and Φ_{Cl^*} consisted of 13 Cl (Cl*) atom profiles obtained in combination with 13 Cl (Cl*) profiles from HCl calibration runs. Experimental errors were determined from the 1σ statistical uncertainties of the experimental data, the uncertainties of the optical absorption cross sections and the uncertainty of the [Cl*]/[Cl] branching ratio value in the 193.3 nm photolysis of HCl using simple error propagation. Values of $\Phi_{Cl} = 0.74 \pm 0.11$ and $\Phi_{Cl^*} = 0.27 \pm 0.03$ were obtained, resulting in a spin-orbit branching ratio of $[Cl^*]/[Cl] = \Phi_{Cl^*}/\Phi_{Cl} = 0.36 \pm 0.08$. From the measured Cl and Cl* atom quantum yields a value of $\Phi_{Cl+Cl^*} = 1.01 \pm 0.14$ can be derived for the total chlorine atom quantum yield in the 193.3 nm photolysis of CH_3CFCl_2.

The absolute primary quantum yield Φ_H for H atom formation in the CH_3CFCl_2 photo-dissociation was determined by calibrating the H atom signal obtained in the CH_3CFCl_2 photo-dissociation against the H atom signal measured in the 193.3 nm photolysis of HCl (see Fig. 3). As in case of the Cl and Cl* quantum yield measurements an absorption correction had to be applied to account for the difference in the absorption cross sections of CH_3CFCl_2 and HCl at the Lyman-α probe laser wavelength.[34] Under the present experimental conditions the absorption correction was $\gamma_H = 0.85 \pm 0.04$. For further details about the calibration procedure are given in Ref. 15. For the absolute H atom quantum yield a value of $\Phi_H = 0.04 \pm 0.01$ was obtained in the evaluation of 8 independent calibration measurements.

B. Average chlorine and hydrogen atom translational energies

Cl, Cl* and H atom Doppler profiles were analysed in order to determine the mean kinetic energy of the respective fragments in the photolysis of CH_3CFCl_2. The Doppler profiles directly reflect, *via* the linear Doppler shift $[\nu - \nu_0] / \nu_0 = v_z / c$, the distribution $f(v_z)$ of the velocity component v_z of the absorbing atoms along the propagation direction of the probe laser beam. As a consequence, for an isotropic velocity distribution the average kinetic energy of the fragments in the laboratory system is given by $E_{T,lab} = 3/2\ m \langle v_z^2 \rangle$. Here $\langle v_z^2 \rangle$ and m represent the second moment of the laboratory velocity distribution $f(v_z)$ and the mass of the photolytically produced atoms, respectively. However, because the measured spectral profiles represent a convolution of the laser spectral profile and the Doppler profile of the absorbing atoms, a numerical deconvolution was applied to obtain the correct fragment velocity distribution $f(v_z)$ employing a Gaussian function to describe the VUV probe laser spectral profile.

In the Cl and Cl* atom formation dynamics studies the evaluation of the 26 recorded Cl and Cl* atom Doppler profiles, taking into account the actual laser bandwidth, yielded values of $E_{T,lab(Cl)} = 107 \pm 8$ kJ/mol and $E_{T,lab(Cl^*)} = 113 \pm 8$ kJ/mol for the mean laboratory kinetic energy of the Cl and Cl* fragments, respectively. For the H atoms produced in the CH_3CFCl_2 photolysis, a value of $E_{T,lab(H)} = 25 \pm 4$ kJ/mol was obtained in the evaluation of the 8 recorded Doppler profiles. The quoted errors include the 1σ statistical uncertainties obtained in the numerical least squares fit analysis of the spectral profiles as well as the respective uncertainties of the laser bandwidth measurements. With the values given above the corresponding mean relative translational energies in the CH_3CFCl + Cl center-of-mass-system were calculated to be $E_{T(Cl)} = 157 \pm 12$ kJ/mol and $E_{T(Cl^*)} = 165 \pm 12$ kJ/mol.

IV. Discussion

A. Primary quantum yield for chlorine atom formation

In principle, the amount of energy provided by a 193.3 nm photon ($\hbar\omega$ = 619.6 kJ/mol) would be high enough to allow for a variety of two-body as well as three-body decay channels for the energized CH_3CFCl_2 molecule (see e.g. Table I). However, as absorption of a 193.3 nm photon actually leads to excitation in the first UV absorption band of CH_3CFCl_2, which originates from a $3p\pi \rightarrow \sigma^*$(C-Cl) transition within the valence shell ($3p\pi$ is a Cl lone pair orbital and σ^* is an antibonding C-Cl σ–MO), one can expect that UV photolysis leads preferentially to breaking of the C-Cl bond. The result of the present absolute quantum yield measurements for chlorine atom formation, $\Phi_{Cl+Cl^*} = 1.01 \pm 0.14$, is in line with this expectation. In addition, because the three-body decay channel in which two chlorine atoms are formed along with the CH_3CF radical is energetically not accessible in the 193.3 nm photolysis of CH_3CFCl_2, the result of the present chlorine atom quantum yield measurement can be directly used to derive an upper limit of $\Phi_{5,..,14} \leq 0.13$[35] for the total quantum yield of the other thermochemically allowed two-body,

$$CH_3CFCl_2 \bullet CH_3CCl_2 + F/F^*, \quad (5)$$

$$CH_3CFCl_2 \bullet CH_2CFCl_2 + H, \quad (6)$$

$$CH_3CFCl_2 \bullet CH_3CF + Cl_2, \quad (7)$$

$$CH_3CFCl_2 \bullet CH_3CCl + ClF, \quad (8)$$

$$CH_3CFCl_2 \bullet CH_2CFCl + HCl, \quad (9)$$

$$CH_3CFCl_2 \bullet CH_2CCl_2 + HF, \quad (10)$$

$$CH_3CFCl_2 \bullet CH_3 + CFCl_2, \quad (11)$$

and three-body decay channels,

$$CH_3CFCl_2 \bullet CH_2CCl + HCl + F/F^*, \quad (12)$$

$$CH_3CFCl_2 \bullet CHCFCl + HCl + H, \quad (13)$$

$$CH_3CFCl_2 \bullet CHCCl_2 + HF + H, \quad (14)$$

which do not result in either Cl or Cl* atom formation.

CH_3CFCl_2 pyrolysis experiments in which the thermal kinetics of the dehydrochlorination channel (9) was studied in the temperature range 610-853 K yielded values of 196.6 kJ/mol[36] and 238.7 kJ/mol[37] for the activation energy of this channel. Only the latter value was found to be consistent with reaction threshold barrier energies of 225.9 kJ/mol and 236.0 kJ/mol obtained in chemical activation experiments[38] and *ab initio* quantum chemical calculations,[39] respectively. With an activation energy of 238.7 kJ/mol, the molecular elimination channel (9) should be energetically accessible in the 193.3 nm photolysis of CH_3CFCl_2. However, the HCl(v = 0, 1) quantum yield of $\Phi_{HCl(v=0,1)} < 0.01$ reported in Ref. 13a along with the fact that no IR emission of HCl(v = 1-4) could be observed following the 193.3 nm photolysis of CH_3CFCl_2[40] indicates that the HCl molecular elimination channel (9) as well as HCl formation *via* the three-body decay channels (12,13) and (15),

$$CH_3CFCl_2 \bullet CH_2CF + HCl + Cl/Cl^*, \quad (15)$$

is only of minor importance in the primary UV photochemistry of CH_3CFCl_2. This parallels the results obtained in the UV photolysis of CH_3CH_2Cl where HCl elimination was also found to be a minor pathway only.[41] HCl formation observed in the 193.3 nm photodissociation of CH_3CH_2Cl

was attributed to a mechanism, which involves internal conversion from the initially electronically excited state(s) to the electronic ground state. The fact that HCl could not be observed in case of CH_3CFCl_2[13a,40] along with the quantum yield for chlorine atom formation of unity — as obtained in the present study — indicates that the dissociation takes place on one (or more) potential energy surface(s), which is (are) repulsive in the C-Cl coordinate and which is (are) not efficiently coupled to the $CH_3CFCl_2(A')$ electronic ground state.[13] In Ref. 14c, based on the analysis of Cl and Cl* photofragment velocity distribution anisotropy parameters β measured in the 235 nm photolysis of CH_3CFCl_2 vibrationally pre-excited to three and four quanta of C-H methyl stretches, it was proposed that electronically excited states of A´ and A´´ symmetry are involved in the UV photodissociation process for excitation energies up to 53761 cm^{-1} (643.9 kJ/mol).

B. C-Cl bond cleavage mechanism, energy disposal, and [Cl*]/[Cl] spin-orbit branching ratio

Although the dynamics of C-Cl bond cleavage has been investigated previously for CH_3CFCl_2 under molecular beam conditions at photolysis wavelengths of 235 and 193.3 nm, no information about the energy disposal was derived in these studies.[13,14a,b] From the Cl and Cl* translational energies obtained in the present 193.3 nm photolysis study translational energy disposal fractions of $f_{T(Cl)} = E_{T(Cl)}/E_{avl} = 0.56$, and $f_{T(Cl^*)} = E_{T(Cl^*)}/E_{avl} = 0.62$, respectively, can be derived employing the respective values of E_{avl} for the two single Cl-bond breaking reaction pathways,

$$CH_3CFCl_2 \bullet CH_3CFCl + Cl, \qquad (16a)$$

$$CH_3CFCl_2 \bullet CH_3CFCl + Cl^*, \qquad (16b)$$

as given in Table I. The present f_T values, which lie between the limiting values 0.36 and 0.85 predicted by a soft impulsive[42] and an impulsive rigid rotor model,[43] demonstrate that C-Cl bond cleavage leads to a rather high translational energy release in the CH_3CFCl_2 photodissociation. The

present results therefore indicate the presence of a prompt dissociation from one or more PESs, which are strongly repulsive in the C-Cl coordinate. A prompt dissociation mechanism, which is consistent with the absence of any structure in the first absorption band of the CH_3CFCl_2 molecule, was also proposed in Ref. 14c to explain the nonvanishing Cl and Cl* photofragment velocity distribution anisotropy parameters β observed in the vibrationally mediated UV photodissociation of CH_3CFCl_2. The present results are in general agreement with the energy disposal fractions observed in the vibrationally mediated 235 nm photolysis of CH_3CFCl_2 ($3\nu_{CH}$) which, with a total excitation energy of 612.9 kJ/mol,[14b] is almost isoenergetic to the 193.3 nm ($\hbar\omega$ = 619.6 kJ/mol) photolysis of vibrational ground-state CH_3CFCl_2. From the Cl and Cl* translational energies given in Ref. 14a, values of $f_{T(Cl)} = 0.44$ and $f_{T(Cl^*)} = 0.51$ can be calculated using the thermochemical data of Table I. The fact that the latter values are somewhat smaller than the present values might be due to the absence of a significant energy flow from the initially excited C-H methyl stretch vibration into the C-Cl bond dissociation coordinate. In Ref. 14c, the experimental observation that the Cl and Cl* product translational energies remained almost constant upon pre-excitation with three, four or even five quanta of C-H methyl stretch was attributed to the rather small amount of additional energy which finally ends up in the C-Cl coordinate after complete energy randomisation among the 18 normal modes of the parent molecule. On the other hand, although C-H methyl stretch pre-excitation was found to be insignificant for the energetics of Cl and Cl* atom formation, a pronounced influence on the overall Cl, Cl* signal strength and on the [Cl*]/[Cl] spin-orbit branching ratio was observed.[13,14a,b] Upon vibrational excitation of the symmetric C-H methyl stretch vibration the spin-orbit branching ratio was observed to increase by about a factor of two from a value of $[Cl^*]/[Cl] = 0.22 \pm 0.06$, as observed in the 193.3 nm ground state photolysis of CH_3CFCl_2 under cold molecular beam conditions ($T_{vib} \approx 100$ K),[13] to a value of $[Cl^*]/[Cl] = 0.49 \pm 0.11$ in the isoenergetic 235 nm photolysis of CH_3CFCl_2 ($3\nu_{CH}$).[14c] In the present 193.3 nm gas-phase photolysis study of room-temperature CH_3CFCl_2 (T = 298 K) an intermediate value of $[Cl^*]/[Cl] = 0.36 \pm 0.08$ was obtained.

As suggested in Ref. 14c, the alteration of the [Cl*]/[Cl] spin-orbit branching ratio upon

vibrational pre-excitation could be due to differences in the improvement of the Franck-Condon (FC) factors relative to the FC factors of the ground state molecules. This in turn could result in an alteration of the ratio of the partial absorption cross sections to the upper PESs involved in the dissociation process of the vibrationally excited molecules. If the [Cl*]/[Cl] spin-orbit branching ratio is determined by the relative strength of the initial absorption cross sections and not significantly altered by subsequent nonadiabatic interactions while the fragments separate, the higher [Cl*]/[Cl] spin-orbit branching ratio observed in the present 193.3 nm room-temperature photolysis study (compared to the 193.3 nm molecular beam photolysis study[13]) could be the result of the markedly different parent molecule vibrational state distributions. For the molecular beam conditions ($T_{vib} \approx 100$ K) one can estimate that only a small fraction (ca. 7%) of the CH_3CFCl_2 molecules are in vibrational levels with $v > 0$, while for the room temperature sample this value is considerably higher (ca. 78%).[44,45]

C. H atom formation dynamics

The H atom quantum yield of $\Phi_H = 0.04 \pm 0.01$ obtained in the present work demonstrates that H atom formation, despite the fact that it could in principle occur *via* a number of reaction channels, such as (6, 13, 14), is only a minor product in the 193.3 nm gas-phase photolysis of CH_3CFCl_2. The present result is in line with the results of previous work in which H atom formation in the dissociation of comparable molecules such as CH_3CF_2Cl,[15] CH_3Cl, and CH_2Cl_2[46] was investigated after photoexcitation in their first absorption bands. In the 193.3 nm gas-phase photolysis of CH_3CF_2Cl an H atom quantum yield of 0.06 ± 0.02 was determined,[15] and even lower H atom quantum yields ($\Phi_H < 0.02$) were observed in case of CH_3Cl, and CH_2Cl_2 at the same photolysis wavelength.

The rather low H atom quantum yield measured in the present work for CH_3CFCl_2 along with the previously reported H atom quantum yields for CH_3CF_2Cl, CH_3Cl, and CH_2Cl_2 show that photoabsorption at 193.3 nm which leads to a $3p\pi \rightarrow \sigma^*$(C-Cl) valence shell transition does not result in efficient primary C-H bond cleavage. However, if these molecules are excited in the VUV

spectral region H atom formation becomes increasingly important.[15,47,48] For CH_3CF_2Cl, for example, it was found that the H atom quantum yield increases from 0.06 ± 0.02 at 193.3 nm to a value of 0.53 ± 0.12 for the Lyman-α photolysis wavelength (121.6 nm).[15] As outlined in Ref. 15, the H atom translational energy release observed in the CH_3CF_2Cl Lyman-α photolysis study along with the results of previous static VUV decomposition experiments indicate that together with H atoms comparable amounts of chlorine atoms and internally excited CH_2CF_2 molecules are produced in the Lyman-α photolysis of CH_3CF_2Cl. For the Lyman-α wavelength, which corresponds to an excitation energy of 985.3 kJ/mol, a Herzberg type I predissociation mechanism[49] was proposed in which a highly excited $CH_3CF_2Cl^{\dagger}$ intermediate, formed by a nonadiabatic transition from the initial excited bound Rydberg state to a dissociative valence state, undergoes a three-body decay to yield CH_2CF_2 + Cl/Cl* + H products. In Ref. 15, it was further noted the latter product channel is already energetically possible in the 193.3 nm photolysis of CH_3CF_2Cl (see Table I of Ref. 15) and the observed H atom Doppler profiles in the 193.3 nm photodissociation dynamics study were found to be consistent with a sequential three-body decay in which the H atoms are produced *via* the "secondary" unimolecular decomposition of the internally excited $CH_3CF_2^{\dagger}$ fragment formed in the "primary" C-Cl bond cleavage process ($CH_3CF_2Cl \rightarrow CH_3CF_2^{\dagger}$ + Cl/Cl*).

In order to access whether the formation of H atoms in the 193.3 nm photolysis of CH_3CFCl_2 *via* a similar three-body decay,

$$CH_3CFCl_2 \bullet CH_2CFCl + Cl/Cl^* + H \qquad (17)$$

would be energetically possible, the kinetic energy distributions of the Cl, Cl* fragments derived from the Doppler profiles measured in the present study were analyzed employing the thermochemical data compiled in Table I. This analysis revealed that in the present case about 12% (corresponding to a fraction of 0.12) of the CH_3CFCl fragments formed *via* the product channels (16a, b) would have enough internal energy to further decompose into H atoms with an average relative translational energy of 25 ± 4 kJ/mol as observed in the present study and CH_2CFCl

molecular fragments, if the latter are formed without internal excitation. The fact that the experimentally observed H versus chlorine atom formation ratio [H]/[Cl + Cl*] = Φ_H / Φ_{Cl+Cl^*} = 0.04 ± 0.02 is about a factor of three lower might indicate that in the actual dissociation mechanism of the three-body decay channel (17) CH_2CFCl fragments are formed with an significant amount of internal excitation.

Although the results of the energy analysis described above show that both the H atom translational energy and the H atom quantum yield of the present work would be consistent with the three-body decay (17), the possibility that H atoms are formed to a certain extend *via* reaction channel (6) or (13, 14) can not be completely ruled out on the basis of the present results. However, in any case an upper limit of $\Phi_{6,13,14,17} \leq 0.05$ can be derived for the total yield of the H atom formation channels (6, 13, 14) and (17) from the upper error bound of the present H atom quantum yield measurement.

"Direct" H atom formation *via* reaction channel (6) was proposed to explain the high H average translation energy of 98 ± 19 kJ/mol which was observed in the 193.3 nm CH_3CFCl_2 molecular beam laser photolysis studies along with a [H]/[Cl + Cl*] branching ratio of 0.18 ± 0.07.[13] For H atoms formed with an average translation energy of 98 kJ/mol, the kinetic energy distributions of the Cl, Cl* fragments as determined in the present work, assuming that under the molecular beam conditions of Ref. 13 the H and the chlorine atoms are formed through the dissociation channel (17), would only allow for a substantially smaller [H]/[Cl + Cl*] branching ratio of ca. 3×10^{-4} even in the limiting case of the CH_2CFCl molecular fragments being formed without any internal excitation. Therefore, it seems to be rather unlikely that the considerable amount of H atoms observed under molecular beam conditions can result from the three-body decay (17). The latter proposition is in line with the conclusion of Ref. 13b where H atom formation *via* the three-body decay (17) was ruled out based on the similarity of the (high) average H atom translational energies observed in the 193.3 nm molecular beam photolysis of CH_3CFCl_2 and CHF_2Cl (for which a three-body decay leading to CF_2 + Cl/Cl* + H is energetically not possible[50]). In addition, in case of the molecular beam photodissociation studies H atom formation

along with HF formation through the three-body decay (14) is also quite unlikely as for this product channel the amount of energy available to the products, E_{avl} = 71.9 kJ/mol, is considerably less than the observed average H atom product translational energy of 98 kJ/mol.

A comparison between the present results obtained in a room-temperature photodissociation study of CH_3CFCl_2 and the results previously obtained under molecular beam conditions suggests that quite different H atom formation mechanisms are operating. While in the room-temperature photolysis relatively "slow" H atoms are formed most probably through a sequential three-body decay (17), in which the H atoms originate from a "secondary" unimolecular decomposition of internally excited CH_3CFCl fragments produced in the "primary" C-Cl bond cleavage reaction (16a, b), the "fast" H atom observed under "cold" molecular beam conditions are more likely to be formed by two-body decay (6) which involves single C-H bond cleavage. Furthermore, internal excitation of the parent molecule seems to have a pronounced influence on the [H]/[Cl + Cl*] branching ratio as indicated by the significant increase from a value of 0.04 ± 0.02 to a value of 0.18 ± 0.07 which is observed upon expansion cooling the parent molecule from room-temperature down to a vibrational temperature of about 100 K. Results of [H]/[Cl + Cl*] branching ratio measurements obtained in the 235 nm molecular beam photolysis of vibrational ground-state and vibrationally pre-excited CH_3CFCl_2, in which the [H]/[Cl + Cl*] branching ratio was found to decrease upon selective C-H methyl stretch excitation (see e.g. the results obtained in the 235 nm photolysis of vibrational ground-state CH_3CFCl_2, $CH_3CFCl_2(3\nu_{CH})$ and $CH_3CFCl_2(4\nu_{CH})$ as reproduced in Table III of Ref. 14b), might be taken as an indication that the markedly different vibrational state distributions in the molecular beam and the room temperature gas phase experiments, which could result in a different Franck-Condon overlap between the ground vibronic and the electronically excited states wavefunctions, are the reason for the observed difference in the [H]/[Cl + Cl*] branching in the 193.3 nm photolysis. However, as already pointed out in Ref. 16 in conjunction with the interpretation of the 193.3 nm room-temperature and molecular beam photolysis results of CH_3CF_2Cl, additional theoretical work is clearly needed both on the involved electronically excited molecular PESs as well as on the molecular dissociation dynamics before it

can be expected that a complete picture of the H atom formation mechanism(s) can be drawn for these molecules. On the experimental side, detailed information on the H atom energy release along with H atom photofragment velocity distribution anisotropy parameter measurements in particular in the vibrationally mediated CH_3CFCl_2 photolysis, for which the reported [H]/[Cl + Cl*] branching ratios indicate that H atom formation becomes a major product channel,[14b,c] would be most helpful to shed more light on the actual dissociation mechanism leading to H atom production.

D. HF formation

Although the formation of HCl in the 193.3 nm photolysis of CH_3CFCl_2 can be ruled out based on experimental results[13a,40] there is no direct experimental evidence indicating the absence of HF formation. On the other hand, preliminary studies on the 193.3 nm gas-phase photolysis of room-temperature CH_3CFCl_2, in which time-resolved Fourier-transform spectroscopy (TRFTS) in the emission mode was applied, seem to indicate that vibrationally exited HF(v = 1-5) photofragments might be produced.[40] Even though HF was not directly detected in the present work, some information about the energetically possible HF formation channels and their relative importance in the 193.3 nm photolysis of CH_3CFCl_2 can be derived from the results of the present Cl, Cl* and H atom photoproduct formation studies.

Based on the thermochemical data compiled in Table I HF could be formed in the 193.3 nm photolysis basically *via* the three-body decay channels (14) and (18),

$$CH_3CFCl_2 \bullet CH_2CCl + Cl/Cl^* + HF \quad (18)$$

as well as *via* the unimolecular 1,2-elimination process (10).[51]

Formation of HF(v = 0, 1) *via* the three-body decay channel (14) would be virtually consistent with the translational energy distribution derived from the H atom Doppler profiles measured in the present study. The analysis of the translational energy distribution revealed that HF(v = 0) formation is energetically possible for 98% of the experimentally observed H atoms.

Also the formation of HF(v = 1) is still possible along with 52% of the observed H atom products. Formation of HF(v > 1), however, would energetically not be allowed. An upper limit of $\Phi_{14} \leq 0.05$ for the quantum yield of HF molecules, which could be formed *via* reaction channel (14), can be derived from the upper error bound of the H atom quantum yield measured in the present work.

In a similar way the possibility for HF formation *via* the three-body decay channel (18) can be assessed by analysing the translational energy distributions of the Cl and Cl* fragments observed in the present experiments. For this channel the analysis showed that HF(v = 0) formation is energetically possible along with up to 66% of the observed Cl and Cl* atoms. From the total chlorine atom quantum yield measured in the present work a value of $\Phi_{18(HF)} = 0.76$ can be obtained for the maximum quantum yield for HF(v = 0) that could be formed.[52] The analysis further revealed that only HF formation up to v = 3 would be energetically allowed for reaction channel (18). Hence, it can be concluded that if HF(v > 3) products are observed they must be formed *via* the elimination channel (10). For the latter channel population of HF vibrational states up to v = 5 as observed in Ref. 40 would be certainly possible considering the high value of the energy available to the products (see Table I).[53,54] Because reaction channel (10) does not result in either Cl or Cl* fragments the upper limit for the total quantum yield for HF formation *via* this channel is restricted by the relationship $\Phi_{10} \leq \Phi_{5,..,14} \leq 0.13$, which (*vide supra*) can be derived from the lower error bound of the present chlorine atom quantum yield measurement.[35]

From the above discussion it is clear that for a more quantitative assessment of the overall importance of HF formation in the UV photodissociation of CH_3CFCl_2 in general and the potential contributions of the three-body decay channels (14, 18) in particular further experimental efforts toward the determination of the [HF(v = 0)] / [HF(v = 1-5)] branching ratio, which could not be provided by the TRFTS studies of Ref. 40, would be required.

V. Summary

In the present gas-phase pulsed laser photolysis/laser-induced fluorescence “pump-and-probe” experiments absolute quantum yields for photolytic formation of Cl, Cl* and H atoms were determined after UV laser excitation of room-temperature CH_3CFCl_2 (HCFC-141b) at 193.3 nm. The value of $\Phi_{Cl+Cl^*} = 1.01 \pm 0.14$ obtained for the total chlorine atom quantum yield along with the rather small H atom quantum yield of $\Phi_H = 0.04 \pm 0.01$ demonstrates that chlorine atom formation is the main photochemical product channel in the 193.3 nm gas-phase photolysis of CH_3CFCl_2 at room temperature. The fractions of total available energy channelled into CH_3CFCl + Cl/Cl* product translational energy was found to be in agreement with results of dynamical simulations employing repulsive models for single C-Cl bond cleavage. The measured total chlorine atom quantum yield and the energy disposal indicate that direct C-Cl bond cleavage on one or more repulsive PESs is the predominant primary fragmentation mechanism for CH_3CFCl_2 after photoexcitation in the first absorption band.

Acknowledgement

The present work was partially supported by the Deutsche Forschungsgemeinschaft (DFG) *via* SFB 359 at the University Heidelberg. AL was supported by the Landesgraduierten Förderung Baden-Württemberg. DS wishes to acknowledge a postdoctoral fellowship provided by the DLR Bonn (Indo-German bilateral agreement, project IND 99/050). HRV would like to thank R. K. Vatsa and P. D. Naik (BARC, Mumbai, India) for many helpful discussions. J. Wolfrum (Director of the Institute of Physical Chemistry, Ruprecht-Karls-University Heidelberg) and J. P. Mittal (Director Chemistry Group, BARC, Mumbai, India) are thanked for their continuous support and interest in the ongoing work.

Figure Caption

Fig. 1 Dependence of the observed Cl (a), Cl* (b) and H atom (c) LIF signal from the CH_3CFCl_2 photodissociation on the 193.3 nm photolysis ("pump") laser intensity I_{pump}. Solid lines are the result of a least-squares fit (I_{pump}^{n}) to the experimental data in order to determine the power-dependence *n* of the respective LIF signals. The values obtained for *n* are given in the figure.

Fig. 2 Doppler profiles of Cl and Cl* (a) atoms produced in the 193.3 nm laser photolysis of 12 mTorr of CH_3CFCl_2 and Cl and Cl* (b) atoms produced in the 193.3 nm laser photolysis of 72 mTorr of HCl. Doppler profiles were recorded 150 ns after the photolysis laser pulse. Line centres correspond to the ($4s\ ^2P_{j'=3/2} \leftarrow 3p\ ^2P_{j''=3/2}$) transition of the Cl atom (74225.8 cm^{-1}) and to the ($4s\ ^2P_{j'=1/2} \leftarrow 3p\ ^2P_{j''=1/2}$) transition of the Cl* atom (73983.1 cm^{-1}), respectively.

Fig. 3 Doppler profiles of H atoms produced in the 193.3 nm laser photolysis of (a) 8 mTorr of CH_3CFCl_2 and (b) 7 mTorr of HCl. Doppler profiles were recorded 100 ns after the photolysis laser pulse. Line centres correspond to the H atom Lyman-α transition (82259 cm^{-1}).

References

[1] E. Linak and P. Yau, *Chemical Economics Handbook* (SRI International, Menlo Park CA, 1995).

[2] D. G. Gehring, D. J. Barsotti, and H. E. Gibbon, J. Chromatogr. Sci. **30**, 301 (1992).

[3] T. Shirai and Y. Makide, Chem. Lett. **4**, 357 (1998).

[4] *Scientific Assessment of Ozone Depletion: 1994*, World Meteorological Organization Report No. 37 (World Meteorological Organization, Geneva, Switzerland, 1995).

[5] Alternative Fluorocarbons Environmental Acceptability Study (AFEAS), "Product, and Sales of Fluorocarbons through 2000" (http://www.afeas.org/production_and_sales.html).

[6] See e.g. R. P. Wayne, *The Chemistry of Atmospheres* 2nd ed. (Oxford Univ. Press: Oxford, 1991); R. Zellner, *Global Aspects of Atmospheric Chemistry* (Springer, New York, 1999) and references therein.

[7] (a) *ATLAS3 Public affairs status report #20*, NASA Science Operation Space Flight Center, Huntsville Nov 13, 1994; (b) S. M. Schauffler, W. Pollock, E. L. Atlas, L. E. Heidt, J. S. Daniel, Geophys. Res. Lett. **22**, 819 (1995); (c) J. M. Lee, W. T. Sturges, S. A. Penkett, D. E. Oram, U. Schmidt, A. Engel, R. Bauer, *ibid.* **22**, 1369 (1995).

[8] (a) R. Warren, T. Gierczak, A. R. Ravishankara, Chem. Phys. Lett. **183**, 403 (1991); (b) R. Atkinson, D. L. Baulch, R. A. Cox, R. F. Hampson, Jr., J. A. Kerr, M. J. Rossi, J. Troe, J. Phys. Chem. Ref. Data **26**, 521 (1997); (c) W. B. DeMore, S. P. Sander, D. M. Golden, R. F. Hampson, M. J. Kurylo, C. J. Howard, A. R. Ravishankara, C. E. Kolb, M. J. Molina, *"Chemical kinetics and photochemical data for use in stratospheric modeling. Evaluation number 12"*, JPL Publication **97-4**, 1 (1997), and references therein.

[9] A. Fahr, W. Braun, M. J. Kurylo, J. Geophys. Res. **98**, 20467 (1993).

[10] R. Talukdar, A. Mellouki, T. Gierczak, J. B. Burkholder, S. A. McKeen, and A. R. Ravishankara, J. Phys. Chem. **95**, 5815 (1991).

[11] R. Warren, T. Gierczak, and A. R. Ravishankara, Chem. Phys. Lett. **183**, 403 (1991).

[12] T. J. Wallington, and M. D. Hurley, Chem. Phys. Lett. **189**, 437 (1992); J. P. Sawerysyn, A. Talhaoui, B. Meriaux, and P. Devolder, Chem. Phys. Lett. **198**, 197 (1992); A. Talhaoui,

F. Louis, P. Devolder, B. Meriaux, J.-P. Sawerysyn, M.-T. Rayez, and J.-C. Rayez, J. Phys. Chem. **100**, 13531 (1996).

13 (a) A. Melchior, I. Bar, and S. Rosenwaks, J. Chem. Phys. **107**, 8476 (1997); (b) A. Melchior, H. M. Lambert, P. J. Dagdigian, I. Bar, and S. Rosenwaks, Isr. J. Chem. **37**, 455 (1997).

14 (a) A. Melchior, X. Chen, I. Bar, and S. Rosenwaks, Chem. Phys. Lett. **315** (1999) 421; (b) J. Chem. Phys. **112**, 10787 (2000); (c) T. Einfeld, C. Maul, K. H. Gericke, R. Marom, S. Rosenwaks, I. Bar, J. Chem. Phys. **115**, 6418 (2001).

15 R. A. Brownsword, M. Hillenkamp, T. Laurent, H.-R. Volpp, J. Wolfrum, R. K. Vatsa, and H.-S. Yoo, J. Chem. Phys **107**, 779 (1997).

16 R. A. Brownsword, P. Schmiechen, H.-R. Volpp, H. P. Upadhyaya, Y. J. Jung, and K.-H. Jung, J. Chem. Phys. **110**, 11823 (1999).

17 A. F. Nayak, T. J. Buckley, M. J. Kurylo, A. Fahr, J. Geophys. Res. **101**, 9055 (1996).

18 G. Hilber, A. Lago, and R. Wallenstein, J. Opt. Soc. Am. B. 4 (1987) 1753.

19 K. Tonokura, Y. Matsumi, M. Kawasaki, S. Tasaki and R. Bersohn, J. Chem. Phys. **97**, 8210 (1992), and references therein.

20 W. L. Wiese, M. W. Smith, and B. M. Miles, Atomic Transition Probabilities, Natl. Bur. Stand. Ref. Data Ser., Natl. Bur. Stand. (U.S.) Circ. No 22 (U.S. GPO, Washington, D.C., 1969).

21 R. A. Brownsword, C. Kappel, P. Schmiechen, H. P. Upadhyaya, and H.-R. Volpp, Chem. Phys. Lett. **289**, 241 (1998).

22 J. P. Marangos, N. Shen, H. Ma, M. H. R. Hutchison, and J. P. Connerade, J. Opt. Soc. Am. B **7**, 1254 (1990).

23 see e.g. R. A. Brownsword, M. Hillenkamp, T. Laurent, R. K. Vatsa, H.-R. Volpp, and J. Wolfrum, J. Chem. Phys. **106**, 1359 (1997).

24 L. A. Curtiss, K. Raghavachari, and J. A. Pople, J. Chem. Phys. **98**, 1293 (1993).

25 M. J. Frisch, G. W. Trucks, H. B. Schlegel, G. E. Scuseria, M. A. Robb, J. R. Cheeseman, V. G. Zakrzewski, J. A. Montgomery, Jr., R. E. Stratmann, J. C. Burant, S. Dapprich, J. M. Millam, A. D. Daniels, K. N. Kudin, M. C. Strain, O. Farkas, J. Tomasi, V. Barone, M. Cossi, R. Cammi, B. Mennucci, C. Pomelli, C. Adamo, S. Clifford, J. Ochterski, G. A. Petersson, P.

Y. Ayala, Q. Cui, K. Morokuma, D. K. Malick, A. D. Rabuck, K. Raghavachari, J. B. Foresman, J. Cioslowski, J. V. Ortiz, A. G. Baboul, B. B. Stefanov, G. Liu, A. Liashenko, P. Piskorz, I. Komaromi, R. Gomperts, R. L. Martin, D. J. Fox, T. Keith, M. A. Al-Laham, C. Y. Peng, A. Nanayakkara, C. Gonzalez, M. Challacombe, P. M. W. Gill, B. G. Johnson, W. Chen, M. W. Wong, J. L. Andres, M. Head-Gordon, E. S. Replogle and J. A. Pople, Gaussian 98 (Revision A.**7**), Gaussian, Inc., Pittsburgh PA, 1998.

26 S.-Y. Chiang, Y.-C. Lee, Y.-P. Lee, J. Phys. Chem. A **105**, 1226 (2001).

27 C. F Melius, Sandia National Laboratories, BAC-MP4 Heats of formation Data file (Version July 6,1996).

28 L. A. Curtiss, K. Raghavachari, P. C. Redfern, and J. A. Pople, J. Chem. Phys. **106**, 1063 (1997).

29 R. J. Berry, D. R. F. Burgess Jr., M. R. Nyden, M. R. Zachariah, and M. Schwartz, J. Phys. Chem J. Phys. Chem. **100**, 1984 (1996).

30 R. J. Berry, D. R. F. Burgess Jr., M. R. Nyden, M. R. Zachariah, C. F Melius, and M. Schwartz, J. Phys. Chem. **100**, 7405 (1996), and references therein.

31 M. W.Chase, Jr., J. Phys. Chem. Ref. Data, Monograph 9 (1998).

32 Y. Mo, K. Tonkua, Y. Matsumi, M. Kawasaki, T. Sato, T. Arikawa, P. T. A. Reilly, Y. Xie, Y. Yag, Y. Huag, and R. J. Gordon, J. Chem. Phys. **97**, 4815 (1992).

33 E. C. Y. Inn, J. Atmos. Sci. **32**, 2375 (1975).

34 R. K. Vatsa, and H.-R. Volpp, Chem. Phys. Lett. **340**, 289 (2001).

35 The upper limit for the total quantum yield of the decay channels (4-10), which do not result in Cl and Cl* formation, is given by 1 - $\underline{\Phi}_{Cl+Cl^*}$ where $\underline{\Phi}_{Cl+Cl^*}$ represents the lower error bound of the present chlorine atom quantum yield measurement ($\underline{\Phi}_{Cl+Cl^*} = 0.87$).

36 D. Sianesi, G. Nelli, and R. Fontanelli, Chim. Ind. (Milan) **50**, 619 (1968).

37 G. Huybrechts, and K. Eerdekens, Int. J. Chem. Kin. **33**, 191 (2001).

38 J. B. McDoniel, and B. E. Holmes, J. Phys. Chem. **100**, 3044 (1996).

39 J. L. Toto, G. O. Prichard, and B. Kirtman, J. Phys. Chem. **98**, 8359 (1994).

40 S.-R. Lin, Y.-J. Chen, S.-C. Lin, and Y. P. Lee, in: *Proceedings of Trombay Symposium on Radiation and Photochemistry*, pp. 315-326 (2000).

[41] M. Kawasaki, K. Kasatani, H. Sato, H. Shinohara, and N. Nishi, Chem. Phys **88**, 135 (1984).

[42] A.F. Tuck, J. Chem. Soc. Faraday Trans. II **73**, 689 (1977).

[43] M. Kawasaki, K. Suto, Y. Sato, Y. Matsumi and R. Bersohn, J. Phys. Chem. **100**, 19853 (1996).

[44] J.R. Durig, C. J. Wurrey, W.E. Bucy, and A. E. Sloan, Spectrochimica Acta **32A**, 175 (1976).

[45] The relative population of the vibrationally excited states was estimated treating the CH_3CFCl_2 molecule as a quantum mechanical harmonic oscillator with 18 normal modes of vibration. The values for the respective vibrational frequencies were taken from Ref. 44.

[46] R. A. Brownsword, M. Hillenkamp, T. Laurent, R. K. Vatsa, H.-R. Volpp, and J. Wolfrum, J. Phys. Chem. A **101**, 5222 (1997).

[47] M.B. Robin, *Higher Excited States of Polyatomic Molecules, Vol. I* (Academic Press, New York, 1974).

[48] R. A. Brownsword, M. Hillenkamp, T. Laurent, R. K. Vatsa, H.-R. Volpp, and J. Wolfrum, J. Chem. Phys. **106**, 1359 (1997).

[49] see e.g. R. Schinke, *Photodissociation Dynamics* (University Press, Cambridge, 1993) and references therein.

[50] A. Melchior, P. Knupfer, I. Bar, S. Rosenwaks, T. Laurent, H.-R. Volpp, and J. Wolfrum, J. Phys. Chem. **100**, 13375 (1996).

[51] HF formation via reaction channel (10) was observed in chemical activation experiments in which internally excited CH_3CFCl_2 molecules were formed by the recombination of CH_3 and $CFCl_2$ radicals.[38] In the latter study, a reaction threshold barrier energy of 284.5 kJ/mol was determined, however, no information regarding the HF product vibrational state distribution in the unimolecular 1,2-elimination process could be obtained.

[52] The upper limit for $\Phi_{18(HF)}$, the quantum yield for HF formation through reaction channel (18), was calculated via $\Phi_{18(HF)} = 0.66 \times \overline{\Phi}_{Cl+Cl^*} = 0.76$, where $\overline{\Phi}_{Cl+Cl^*}$ represents the upper error bound of the present chlorine atom quantum yield measurement ($\overline{\Phi}_{Cl+Cl^*} = 1.15$). The value 0.66 represents the fraction of the Cl and Cl* atoms which can be formed along with

HF(v = 0).

53 Formation of HF up to v = 5 was previously observed in the 193.3 nm photolysis of CH_2CF_2 (Ref. 54a) and CH_2CFCl (Ref. 54b) where the amount of energy available to the products of the respective HF elimination channels are comparable to that of the HF elimination channel (10) in the 193.3 nm photolysis of CH_3CFCl_2.

54 (a) G. E. Hall, J. T. Muckerman, J. M. Preses, R. E. Weston, Jr., G. W. Flynn, and A. Persky, J. Chem. Phys. **101**, 3679 (1994); (b) T. R. Fletcher, and S. R. Leone, J. Chem. Phys. **88**, 4720 (1988).

55 I. Barin, *Thermochemial Data for Pure Substances* (VCH, Weinheim, 1995).

56 J. A. LaVilla, J. L. Goodman, J. Am. Chem. Soc. **111**, 6877 (1989).

57 M. Mansson, B. Ringner, and S. Sunner, J. Chem. Thermodyn. **3**, 547 (1971).

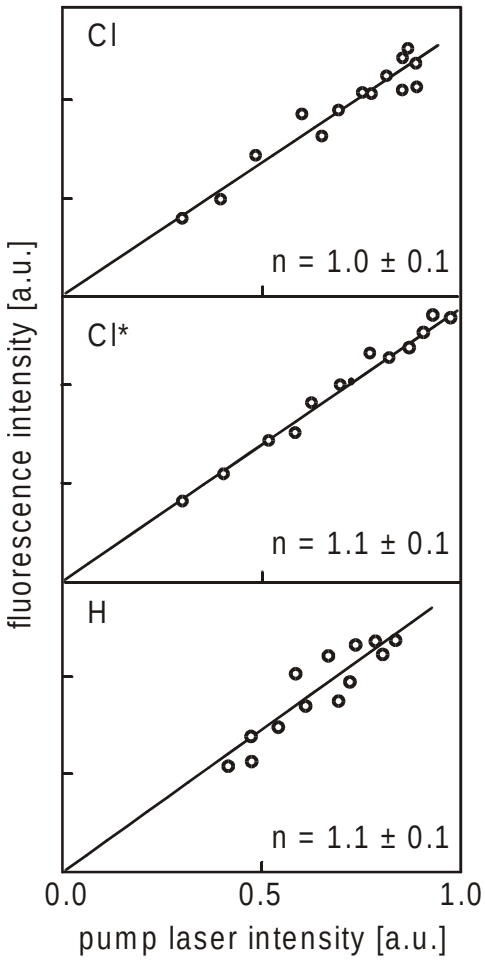

Fig.1 Läuter et al.

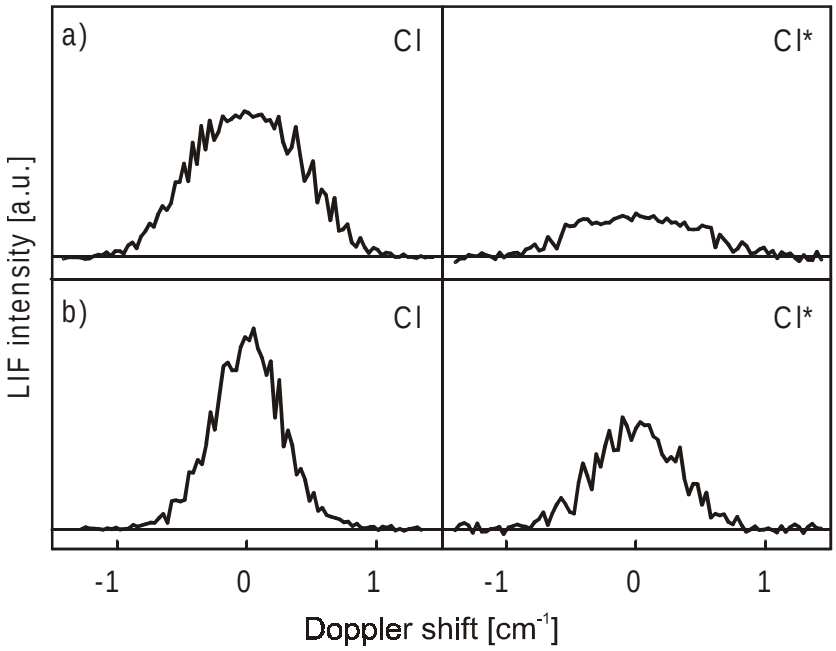

Fig.2 Läuter et al.

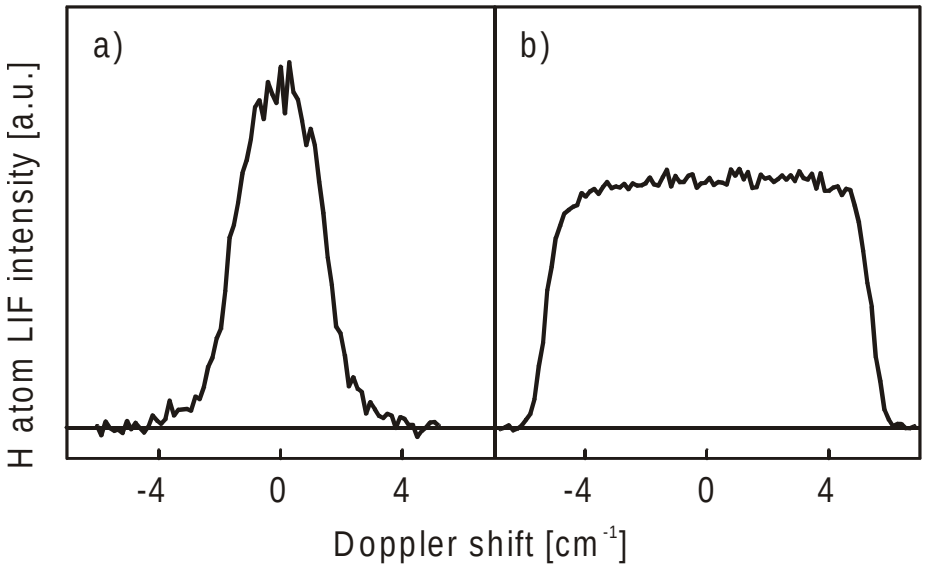

Fig.3 Läuter et al.

Table I. Standard enthalpies of formation, $\Delta_f H^o_{298}$, and reaction enthalpies, $\Delta_r H^o_{298}$, of energetically accessible photochemical product channels in the 193.3 nm photolysis of CH_3CFCl_2. Energies available to the respective products, E_{avl}, were calculated *via* $E_{avl} = \hbar\omega_{pump}(193.3\ nm) - \Delta_r H^o_{298}$. Energies are given in kJ/mol.

Species	$\Delta_f H^o_{298}$	Ref.	Product channel	$\Delta_r H^o_{298}$	E_{avl}
CH_3CFCl_2	-339.2	(*)	$CH_3CFCl_2 \rightarrow CH_3CFCl + Cl$	341.4	278.3
CH_3CFCl	-119.1	(*)	$CH_3CFCl_2 \rightarrow CH_3CFCl + Cl^*$	352.0	267.7
CH_3CCl_2	43.2	[27]	$CH_3CFCl_2 \rightarrow CH_2CFCl_2 + H$	449.0	170.7
CH_2CFCl_2	-108.2	[27]	$CH_3CFCl_2 \rightarrow CH_3CCl_2 + F$	461.8	157.9
CH_2CFCl	-165.4	[55]	$CH_3CFCl_2 \rightarrow CH_3CCl_2 + F^*$	466.6	153.1
CH_3CCl	212.0	[56]	$CH_3CFCl_2 \rightarrow CH_2CFCl + HCl$	81.5	538.2
CH_3CF	67.9	[27]	$CH_3CFCl_2 \rightarrow CH_2CCl_2 + HF$	69.0	550.7
CH_2CCl_2	2.2	[57]	$CH_3CFCl_2 \rightarrow CH_3CCl + ClF$	500.9	118.8
CH_2CCl	257.0	[27]	$CH_3CFCl_2 \rightarrow CH_3CF + Cl_2$	407.1	212.6
CH_2CF	109.1	[27]	$CH_3CFCl_2 \rightarrow CH_3 + CFCl_2$	389.7	230.0
$CHCCl_2$	260.7	[27]	$CH_3CFCl_2 \rightarrow CH_2CFCl + Cl + H$	513.1	106.6
$CHCFCl$	77.8	(*)	$CH_3CFCl_2 \rightarrow CH_2CFCl + Cl^* + H$	523.7	96.0
$CFCl_2$	-95.2	[27]	$CH_3CFCl_2 \rightarrow CH_2CF + Cl + HCl$	477.3	142.4
CH_3	145.7	[31]	$CH_3CFCl_2 \rightarrow CH_2CF + Cl^* + HCl$	487.9	131.8
ClF	-50.3	[31]	$CH_3CFCl_2 \rightarrow CH_2CCl + Cl + HF$	445.1	174.6
HCl	-92.3	[31]	$CH_3CFCl_2 \rightarrow CH_2CCl + Cl^* + HF$	455.7	164.9
HF	-272.4	[31]	$CH_3CFCl_2 \rightarrow CH_2CCl + F + HCl$	583.3	36.4
F/F*	79.4/84.2	[31]	$CH_3CFCl_2 \rightarrow CH_2CCl + F^* + HCl$	588.1	31.6
Cl/Cl*	121.3/131.6	[31]	$CH_3CFCl_2 \rightarrow CHCFCl + H + HCl$	542.7	77.0
H	218.0	[31]	$CH_3CFCl_2 \rightarrow CHCCl_2 + H + HF$	545.5	74.2

(*) values obtained in the present work from G2(MP2) calculations employing different isodesmic reaction schemes (details are given in the text).